Physical properties of spray pyrolysed ZnO thin films obtained from nitrate, acetate and chloride precursors: Comparative study for Solar Cell Applications

K. Salim[a,*] and W. Azzaoui[b]

[a] *Scientific and technical information research centre, embedded systems research unit, Chlef, CERIST, 02000, Algeria.*

[*] *e-mail: karim22000@hotmail.com; skarim@cerist.dz*

[b] *Materials Development and Characterization Laboratory, Department of Electronics, Djillali Liabes University, BP89, Sidi Bel Abbes 22000, Algeria.*

Received 8 July 2022; accepted 6 September 2022

ZnO thin films prepared using zinc chloride, zinc acetate and zinc nitrate precursors have been successfully synthesized by Spray Pyrolysis method. Films depositions were carried out on glass substrates at 350°C. Structural properties of ZnO films were investigated by X-ray diffraction (XRD), confirming that all precursors have an Hexagonal Wurtzite structure. The obtained films were oriented along the preferential (002) crystallographic plane. The phase purity was also confirmed by X-ray photoelectron spectroscopy (XPS), Ultra Violet-Visible, and Energy Dispersive X-ray spectroscopy measurements (EDX). The optical measurement revealed that films have average transmittance of 58%, 78% and 65% for zinc chloride, zinc acetate and zinc nitrate, respectively. The band gap values obtained are 3.19, 3.17 and 3.23 eV for ZnO films using zinc acetate, zinc chloride and zinc nitrate precursors, respectively. Additionally, the refractive index and extinction coefficient of the ZnO films for all precursors have been explored.

Keywords: ZnO; thin films; spray pyrolysis.

DOI: https://doi.org/10.31349/RevMexFis.69.031002

1. Introduction

Zinc oxide (ZnO) is a n-type compound semiconductor with a direct wide band gap [1]. It has a relatively large exciton binding energy (60 meV) at room temperature [2], good optical properties and a high stability [3]. Zinc oxide represents an important basic material due to its low cost as well as its electrical, optoelectronic and luminescent properties [4]. Overall, ZnO is of importance for fundamental research, and also relevant for various fields of industrial and high technological applications such as gas sensors [5], varistors [6], piezoelectric [7], UV light detector and Schottky diodes [8]. Various ZnO nanostructures, such as nanorods have been fabricated by thermal evaporation [9], chemical vapor deposition [10], sol-gel method [11], electrochemically deposition, ion beam assisted deposition [12], rf magnetron sputtering deposition [13], metalorganic chemical vapor deposition [14] and spray pyrolysis aqueous solution method [15]. Among these methods, pulverized pyrolysis is particularly suitable and useful for large surface applications, as it has proven to be a simple and inexpensive method. Many authors have described the preparation of ZnO thin films using spray pyrolysis. However, little attention has been paid to the character of precursors such as Romero *et al*. [16]. In the present study, by using the spray pyrolysis technique, we report a comparative study of different precursors such as zinc acetate, zinc chloride and zinc nitrate on the ZnO thin films. The structural and optical properties were also investigated.

2. Experimental details

The ZnO thin films for all precursors were fabricated by the chemical spray pyrolysis spray technique on glass substrates. Before the deposition, the substrates of dimensions 75×25 mm^2 were cleaned with acetone and double-distilled water.

The chemical precursors used are zinc acetates (Zn $(CH_3COO)_2.2H_2O$), zinc chloride ($ZnCl_2.H_2O$) and zinc nitrates (Zn $(NO_3)_2.6H_2O$). These chemicals were dissolved in double-distilled water at the 0.1 M concentration. Note that a small amount of hydrochloric acid (HCl) has been added to dissolve the zinc chloride since it gives a chemical precipitate if only double-distilled water is used to dissolve it.

Furthermore, all the thin ZnO films obtained were manufactured under the same conditions summarized in Table I.

TABLE I. Conditions for depositing thin films of ZnO.

Chemical precursors	zinc acetate (Zn (CH3COO)$_2$.2H$_2$O) zinc chloride (ZnCl$_2$.H$_2$O) zinc nitrate (Zn (NO$_3$)2 .6H$_2$O)
Substrate used	Laboratory glass
Deposit temperature	$350 \pm 10^{\circ}$C
Distance between substrate and hotplate	30 cm
Spray solution flow rate	2 ml /min
Volume of sprayed solution	50 ml

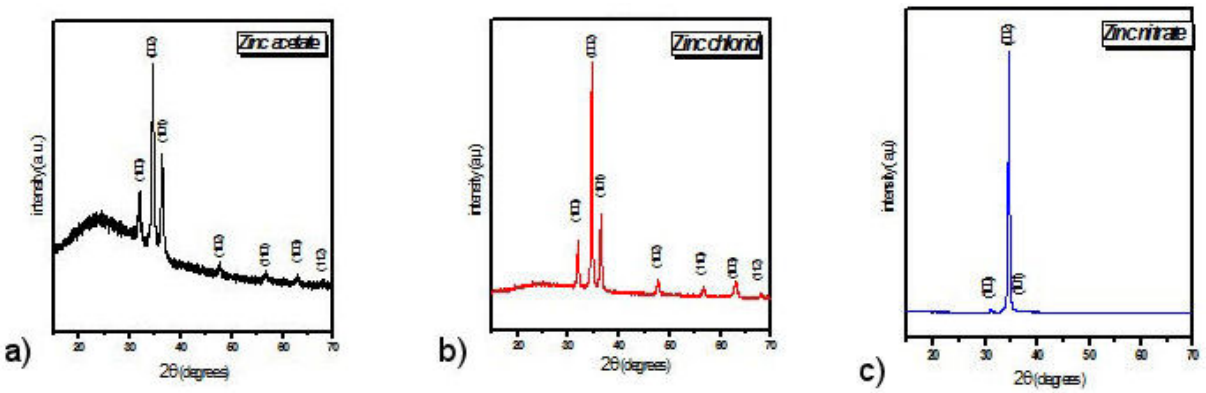

FIGURE 1. XRD spectra of fabricated ZnO thin films.

3. Results and discussion

3.1. Structural properties and morphology

The structural characterization was performed at room temperature using a Bruker X-ray diffractometer model D2 Phaser with CuKα radiation ($\lambda = 1.5406$ Å).

Figure 1 shows the XRD diffraction spectra of ZnO thin films obtained using zinc acetates (Fig. 1a), zinc chloride (Fig. 1b) and nitrates of zinc (Fig. 1c) as precursors.

The comparison of its XRD spectra with the standard card JCPDS (Joint Committee on Powder Diffraction Standards) $N°$36-1451 [17-19] allowed us to conclude that these are polycrystalline thin films of ZnO crystallized in the hexagonal Wurtzite phase.

After indexing its spectra according to the data available in the JCPDS map $N°$36-1451 (angular positions of the peaks and their corresponding hkl indices), it was noticed that the thin ZnO films obtained using zinc acetates present several reflecting planes, (100), (002), (101), (102), (110), (103) and (112) with a fairly high background noise compared to the maximums of the intensities of reflective peaks. This means that in the case where there are several reflecting planes, this material is not well crystallized, this is the case with the thin films of ZnO obtained from acetates, there is coexistence of the amorphous ZnO material and ZnO crystallites oriented along the planes cited above. The shape of the diffraction spectrum recorded for the ZnO films obtained from acetates also means that there is no strong preferential orientation for the crystallites within them.

Regarding the thin ZnO films obtained from zinc chloride, the indexing of their corresponding XRD spectrum (Fig. 1b), indicates the presence of the same reflective planes observed in the XRD spectrum relating to the films ZnO obtained from acetates, namely (100), (002), (101), (102), (110), (103) and (112). However, unlike the films obtained from zinc acetates, the XRD spectrum relating to those obtained from zinc chloride presents a background noise (Backgound) low in intensity compared to the intensities of the peaks corresponding to the reflecting planes, meaning that amorphous composition is present in these films. Furthermore, a weak preferential orientation of ZnO crystallites with ZnO thin films obtained from zinc chloride as well as those obtained from acetates.

The examination of the XRD diffraction spectrum, relating to the thin ZnO films obtained from zinc nitrates, is characterized by the presence of three peaks corresponding to the reflecting planes (110), (002) and (101) with a noise of almost zero bottom if one compares its intensity compared to that of the peak (002). Furthermore, the intensities of the peaks recorded show a strong preferential orientation along the crystallographic plane [002], noted as the c axis which is perpendicular to the growth plane (plane of the substrate). This result shows that the crystallites composing the thin ZnO films obtained from nitrates grow more easily along the c axis which can be characterized as being the axis relating to the minimization of internal stresses and surface energy [20]. The grain sizes, lattice constants, strains and dislocation density have been evaluated according to Fig. 3. For the estimation of crystallite size the Sherrer formula is used [21,22]:

$$D = \frac{0.9\lambda}{\beta \cos\theta}, \tag{1}$$

where $k = 0.9, \lambda = 1.5406$ Å is the x-ray wavelength, β is the full width at half maximum (FWHM) of the XRD peak, and θ is Bragg's diffraction angle. The lattice parameters of the films are determined by the following relation [23]:

$$\frac{1}{d^2hkl} = \frac{4}{3}\left(\frac{h^2 + hk + k^2}{a^2}\right) + \left(\frac{l^2}{c^2}\right). \tag{2}$$

The micro-strain (ε) has been estimated using the following formula [24]:

$$\varepsilon = \frac{\beta \cos\theta}{4}. \tag{3}$$

The dislocation density of the films has been estimated using the following formula [24]:

$$\delta = \frac{1}{D^2}. \tag{4}$$

All the structural parameters, *i.e.*, full width at half maximum (FWHM), crystallite sizes, lattice constants (a and c), strains and dislocation density are summarized in Table II.

TABLE II. Structural parameters of fabricated ZnO thin films.

Samples	$2\theta^\circ$ (002)	FWHM $.10^{-3}$ (Degrees)	Crystallite size (nm)	a (A°)	c (A°)	Strain (10^{-4})	Dislocation density (10^{-4} Line/nm^2)
JCPDS card N° 36-1451	34.422	-	-	3.24	5.20	-	-
zinc acetate	34.432	5.562	25.157	3.23	5.19	13.778	15.789
zinc chloride	34.574	5.460	26.595	3.23	5.19	13.033	14.138
zinc nitrate	34.521	5.093	28.508	3.24	5.19	12.157	12.300

According to Table II, the values of the calculated lattice parameters (a and c) are in agreement with those of standard ZnO (JCPDS card N° 36-1451) and those reported in the literature [26]. Moreover, the sizes of the crystallites oriented along the crystallographic plane (002) which constitute the three films of ZnO have the same order of magnitude with a slight difference and consistency with the results found by other researchers [27]. In fact, it is noted that the ZnO films obtained from zinc nitrates have the smallest size relative to those obtained from acetates and chloride. On the other hand, it is noted that the meshes of the crystallites oriented according to [002] undergo deformation stresses which are the least important for the ZnO films made from nitrates which also result in the lowest density of dislocations (Table II) and consequently fewer structural defects compared to ZnO films obtained from the other zinc acetate and zinc chloride precursors.

3.1.1. Calculation of crystallinity

During the development of polycrystalline thin films, the growth of the material on amorphous substrates, in this case glass, is not favored according to any precise crystallographic orientation plane. Often, and for thermodynamic reasons (energy of formation, temperature etc.), the growth of the material takes place in a mixture of crystalline and amorphous or even totally amorphous (disordered growth).

In this sense, the films obtained can be characterized by a parameter (the amount of amorphous material) that can inform us about their crystalline quality, thus indicating the amorphous and crystalline fractions that make up the samples thus obtained. Experimentally, the amorphous state of a given material results in the recording of a diffraction spectrum with a very broad peak at all angles 2θ scanned. This is clearly seen in the spectrum of Fig. 2d), relating to the glass we used as a deposition support for our films.

Moreover, when a polycrystalline layer is involved, in this case the manufactured ZnO thin films, their diffraction spectra are made up of both an amorphous part, which is distinguished by a large envelope, often called background, and very distinct peaks positioned at very precise angles (Fig. 2a), b) and c)) relating to the reflective planes characteristic of the crystallographic orientation planes of the crystallites that make up the layer.

The percentage of the amount of amorphous or disordered material in the sample is defined by the expression [25]: $\% = S_G - S_{pc}/S_G$ with S_G the overall area of the diffraction spectrum surface of the curve, and S_{pc} the surface area of the crystal peaks.

Therefore, subtracting this percentage from the amount of amorphous material in 100 gives the amount of crystallised material in the sample commonly referred to as 'crystallinity': % of the amount of crystalline material = 100 - % of the amount of amorphous material. The results of the calculation performed using the Eva-Diffrac software [26] are given in Table II.

It is clear from Table II that the ZnO samples obtained using the zinc nitrate precursor have a much higher crystallinity than the ZnO samples obtained from the zinc acetate and zinc chloride precursors. This indicates that the ZnO films obtained from the nitrates have good crystallinity compared to those obtained from the other two precursors.

Note that in the calculation of the results summarized in Table II, the contribution of the glass substrate in the diffraction spectra has been neglected. This approximation is all the more plausible if we consider medium thick films, which is the case in our experiment.

The analyses of chemical composition were carried out using a Jeol JSM 5800 scanning electron microscope which is equipped with energy dispersive X-ray detector (EDX, IXRF Model 550i). The XPS measurements were carried out on a Kratos Axis Ultra using Al Kα (1486.6 eV) radiation. High resolution spectra were acquired at 20 eV pass energy with energy resolution of 0.9 eV. The C1 s line of 284.5 eV was used as a reference to correct the binding energies for charge energy shift.

TABLE III. Crystallinity rates of the ZnO samples obtained.

ZnO thin films	Crystallinity (%)	Amorphous composition
Obtained from Acetates	9.6	90.4
Obtained from Chlorides	22.4	77.6
Obtained from Nitrate	82.4	17.6

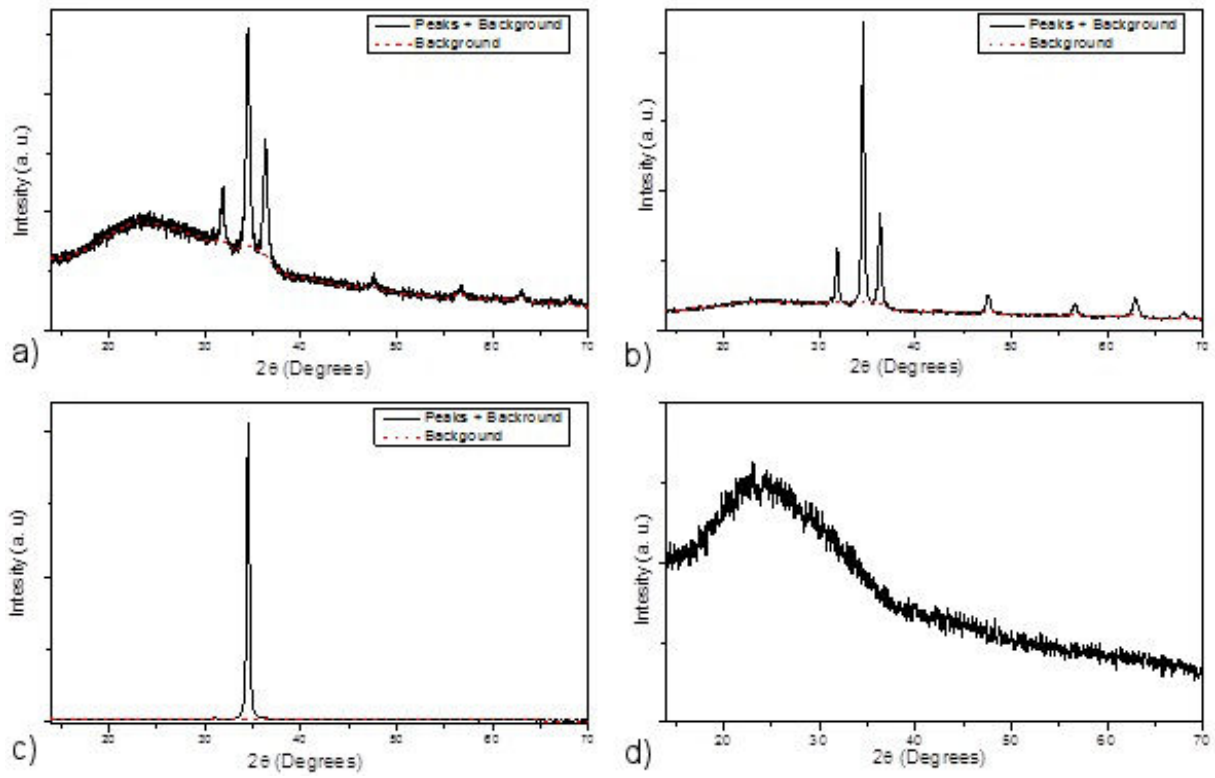

FIGURE 2. XRD diffraction spectra and background adjustment. a) XRD spectrum of ZnO films obtained from Acetates; b) XRD spectrum of ZnO films obtained from Chlorides; c) XRD spectrum of ZnO films obtained from Nitrates ; d) XRD spectrum of the glass substrates used.

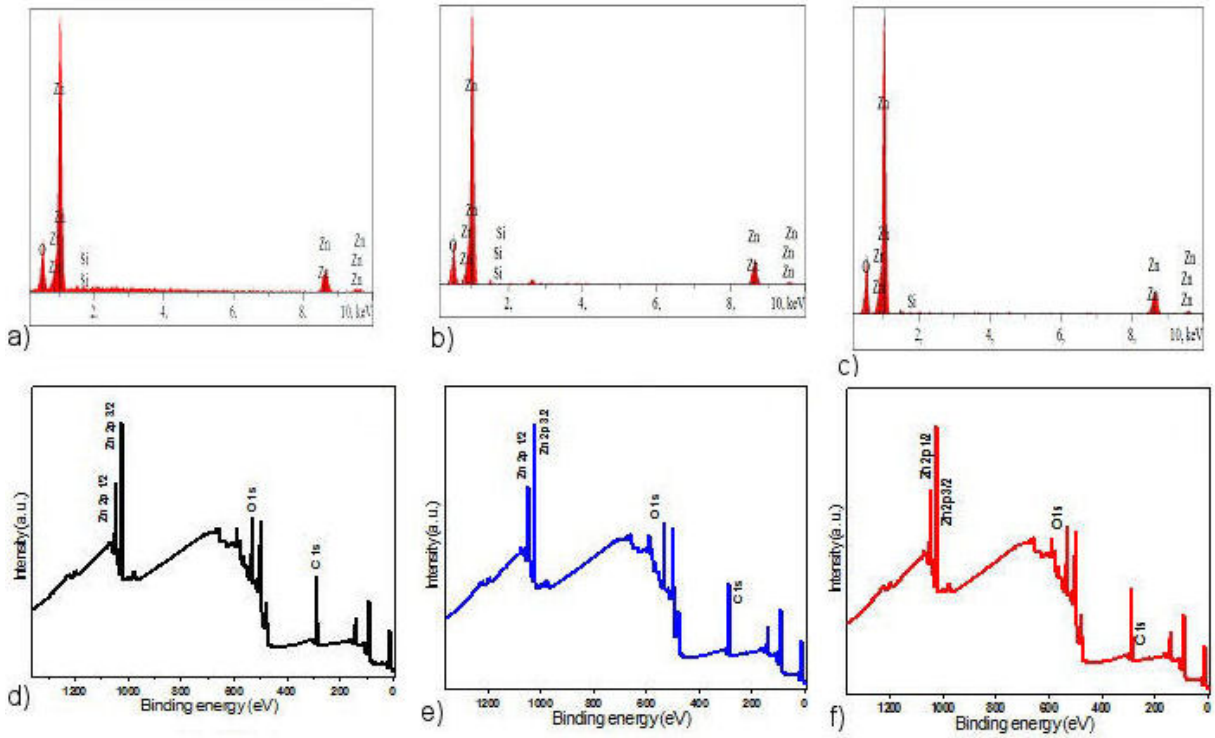

FIGURE 3. a)-c) Energy dispersive X-ray (EDX) spectra, d)-f) XPS full survey scan of the obtained zinc acetate, zinc chloride and zinc nitrate, respectively.

The chemical composition checking by the EDX spectra is given in Fig. 3a). As expected, EDX spectra show the presence of peaks attributed to zinc and oxygen elements for all samples and reveal the presence of silicon attributed to the glass substrate.

Figure 3b) illustrates the general (XPS) spectrum of the ZnO obtained from zinc acetate, zinc chloride and zinc nitrate, respectively. It can be observed that the Zinc, Oxygen and Tin peaks are presented, which confirms the (EDX) and (XRD) analysis previously done.

3.2. Optical properties

The optical transmittances have been recorded between 200 and 2500 nm wavelength using a JASCO 570 type UV-vis-NIR double-beam spectrophotometer. Figures 4a)-c) show the optical spectra for ZnO thin films obtained by using different precursors such as zinc acetate (Fig. 4a)), zinc chloride (Fig. 4b)) and zinc nitrate (Fig. 4c)). The optical transmission spectra of the ZnO thin films using the above mentioned precursors were not found to be highly transparent. In the case of thin films of ZnO manufactured using the precursor zinc nitrates, it is noted that the average transmission in the visible range is around 65% (Fig. 4c)) which is in agreement with the work of A. Nakrela *et al.* [28]. This relatively high transparency is attributed to their good crystallinity, unlike the thin ZnO films obtained from zinc acetates and zinc chloride which have lower transmittances of the order of 58% and 61%, respectively, in agreement with the work of H. Benzarouk *et al.* [29]. We note, moreover, the absence of interference fringes in the recorded transmission spectra, which may be due to the roughness of the surface of the films deposited by spray pyrolysis due to the small size of the droplets of the solutions [29].

The band gap of thin ZnO films is an important parameter for estimating the limit of their absorption band. The optical band gap was determined using the following formula [30-32]:

$$(\alpha h\nu)^n = A(h\nu - Eg), \tag{5}$$

where α is the absorption coefficient, $h\nu$ the photon energy, A, a relation constant and Eg the optical band gap. We have usually taken $n = 0.5$ for indirect band gap semiconductors and $n = 2$ for direct band gap semiconductors. As ZnO no is considered as a direct semiconductor, the intersection of the extrapolation of the linear region of $(\alpha h\nu)^2$ on the energy axis makes it possible to determine the optical gap (Fig. 5). It can be observed that the gap values for ZnO

lms using zinc acetates, zinc chlorides and zinc nitrates are 3.19, 3.17, and 3.23 eV, respectively,nin agreement with the results of the literature [33].

The refractive index n, extinction coefficient k and the thickness d of the thin films were estimated with the spPS (seed preprocessing Pattern search) technique[34]. The obtained values of the deposited films thicknesses are 282, 299, 291 (nm) for ZnO obtained from acetates, chloride and nitrates respectively The refractive index n (Fig. 6a) and the value of extinction coefficient k (Fig. 6b) varied from 2.13

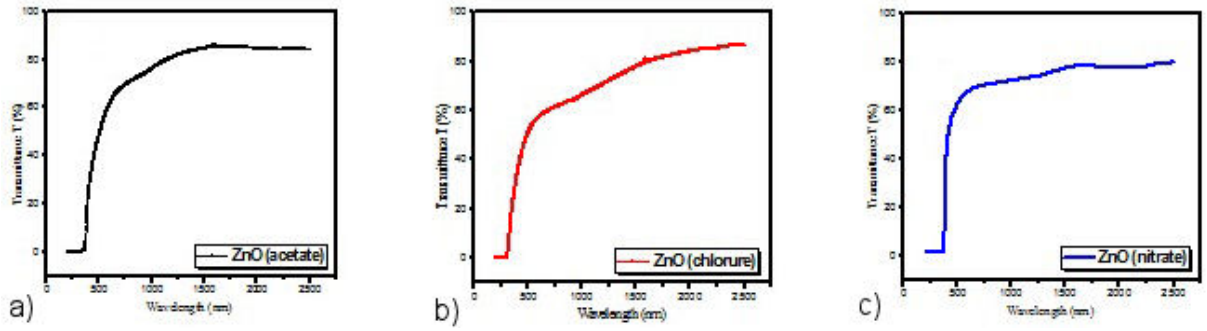

FIGURE 4. Transmittance spectra of manufactured ZnO thin films. a) zinc acetate; b) zinc chloride; c) zinc nitrate.

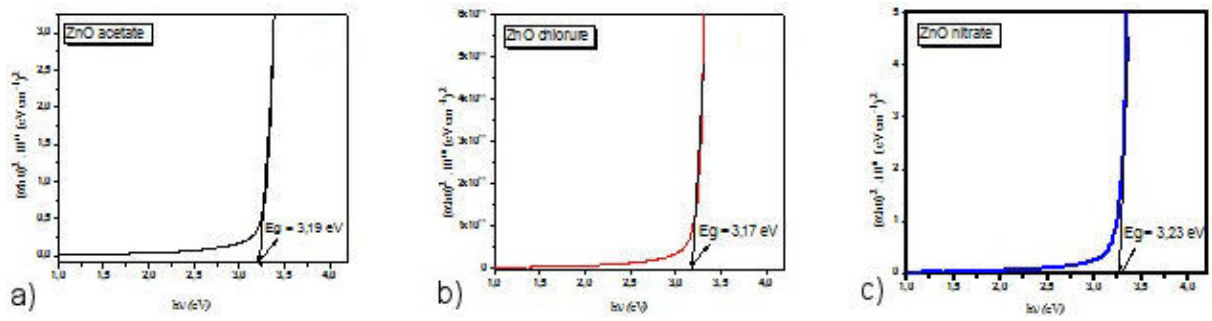

FIGURE 5. Variation of $(\alpha h\nu)^2$ as a function of the energy of ZnO thin films. a) zinc acetate; b) zinc chloride; c) zinc nitrate.

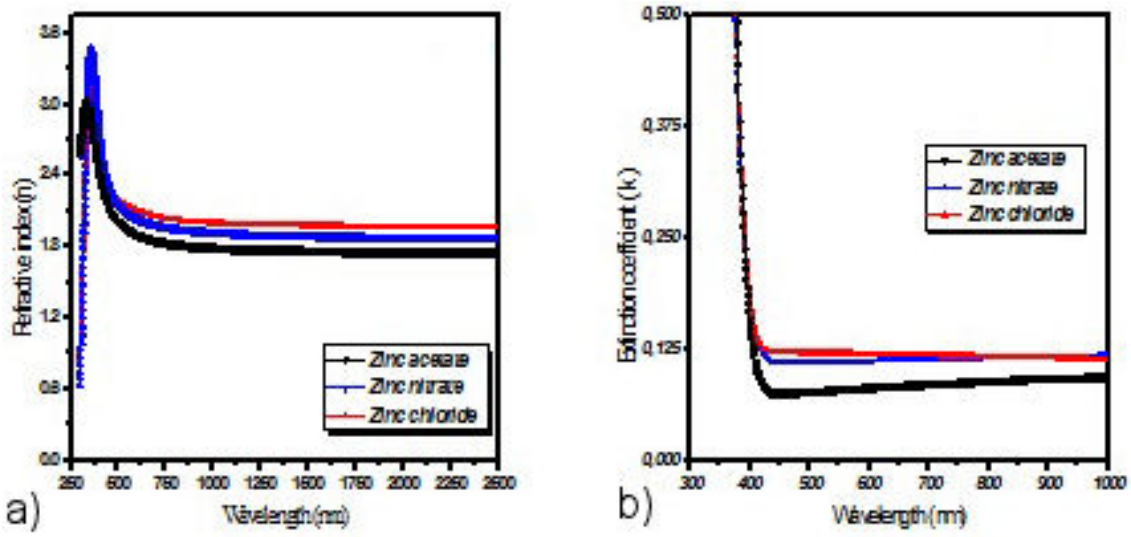

FIGURE 6. The refractive index a), and extinction coefficient b) of the films obtained with zinc acetate, zinc chloride and zinc nitrate, respectively.

to 1.8, and from 0.12 to zinc acetate, zinc chloride and zinc nitrate, respectively in the visible wavelength range. Similar values are observed in Refs. [15,22,33]. These films with low values of n and k are recommended for optoelectronic device applications such as solar cell window films [35,36].

4. Conclusion

ZnO thin films were prepared using zinc acetate, zinc chloride and zinc nitrate precursors by spray pyrolysis technique on glass substrates at $350°$C. ZnO thin films are all in hexagonal structure. The film grown using zinc nitrate precursor had a well-preferred orientation of (002) while the other two are low oriented. The EDX images and XPS spectra for all samples confirmed the deposition of Zn and O in the films, and the EDX pattern validated the XRD result. The optical measurements revealed that films have a low transmittance of the zinc acetate and zinc chloride around 58% and 61%, respectively. On the other hand the zinc nitrate achieved 65%. The calculated optical band gap values are 3.19, 3.17 and 3.23 eV for ZnO using different precursors of zinc acetate, zinc chloride and zinc nitrate, respectively. This study suggests that the ZnO obtained from nitrate is the preferable one candidate for optoelectronic applications such as photovoltaic solar cells.

1. K. Salim and M. N Amroun, Study of the Effects of Annealing Temperature on the Properties of ZnO Thin Films Grown by Spray Pyrolysis Technique for Photovoltaic Applications, International *Journal of Thin Film Science and Technology* **11** (2022) 19, https://dx.doi.org/10.18576/ijtfst/110103.

2. K. Salim, *et al.*, Enhancement of optical and electrical properties of spray pyrolysed ZnO thin films obtained from nitrate chemical by Al-Sn co-doping, *Optik* **210** (2020) 164504, https://dx.doi.org/10.1016/j.ijleo.2020.164504.

3. K. Salim, *et al.*, Effect of Mn Doped and Mn+ Sn Co-doping on the Properties of ZnO Thin Films, International Journal of *Thin Film Science and Technology* **10** (2021) 233, https://dx.doi.org/10.18576/ijtfst/100313.

4. K. Salim and M. N Amroun, Improved Physical Properties of ZnO Films with a second Superposed SnO2 very Thin Films Deposited by Spray Pyrolysis Method, *International Journal of Thin Film Science and Technology* **11** (2022) 29, https://dx.doi.org/10.18576/ijtfst/110104.

5. R. Mariappan, *et al.*, Role of substrate temperature on the properties of Na-doped ZnO thin film nanorods and performance of ammonia gas sensors using nebulizer spray pyrolysis technique, *Journal of alloys and compounds* **582** (2014) 387, https://doi.org/10.1016/j.jallcom.2013.08.048.

6. K. Hembram, *et al.*, High performance varistors prepared from doped ZnO nanopowders made by pilot-scale flame spray pyrolyzer: Sintering, microstructure and properties, *Journal of the European Ceramic Society* **35** (2015) 3535, https://doi.org/10.1016/j.jeurceramsoc.2015.05.035.

7. Q. Fan, *et al.*, Structure and piezoelectricity properties of V-doped ZnO thin films fabricated by sol-gel method, *Journal of Alloys and Compounds* **829** (2020) 154483, https://doi.org/10.1016/j.jallcom.2020.154483.

8. D. H. Vieira, *et al.*, UV-photocurrent response of zinc oxide based devices: Application to ZnO/PEDOT: PSS hydrid Schottky diodes, *Materials Science in Semiconductor Process-*

ing **121** (2021) 105339, https://doi.org/10.1016/j.materresbull.2020.105339.

9. N. Sheeba, *et al.*, Studies on Photoresponse and LPG sensitivity of transparent Al doped ZnO thin films prepared by thermal evaporation technique, *Materials Research Bulletin* **93** (2017) 130, https://doi.org/10.1016/j.materresbull.2017.04.021.
10. Y. Y. Villanueva, D.-R. Liu, and P. T. Cheng, Pulsed laser deposition of zinc oxide, *Thin Solid Films* **501** (2006) 366, https://doi.org/10.1016/j.tsf.2005.07.152.
11. S. Ilican, *et al.*, Temperature dependence of the optical band gap of sol-gel derived Fe-doped ZnO films, *Optik* **127** (2016) 8554, https://doi.org/10.1016/j.ijleo.2016.06.074.
12. I. N. Reddy, *et al.*, Effect of seed layers (Al, Ti) on optical and morphology of Fe-doped ZnO thin film nanowires grown on Si substrate via electron beam evaporation, *Materials Science in Semiconductor Processing* **71** (2017) 296, https://doi.org/10.1016/j.mssp.2017.08.015.
13. T. Yang, *et al.*, Transparent conducting ZnO: Al films deposited on organic substrates deposited by rf magnetron-sputtering, *Thin solid films* **326** (1998) 60, https://doi.org/10.1016/S0040-6090(98)00763-9.
14. Y. Liang, Chemical vapor deposition synthesis of Ge doped ZnO nanowires and the optical property investigation, *Physics Letters A* **383** (2019) 2928, https://doi.org/10.1016/j.physleta.2019.06.024.
15. A. Bedia, *et al.*, Structural, electrical and optical properties of Al-Sn codoped ZnO transparent conducting layer deposited by spray pyrolysis technique, *Superlattices and Microstructures* **111** (2017) 714, https://doi.org/10.1016/j.spmi.2017.07.031.
16. R. Romero, *et al.*, The effects of zinc acetate and zinc chloride precursors on the preferred crystalline orientation of ZnO and Al-doped ZnO thin films obtained by spray pyrolysis, *Thin Solid Films* **515** (2006) 1942, https://doi.org/10.1016/j.tsf.2006.07.152.
17. Ü. Alver, A. Kudret, and S. Tekerek, Spray pyrolysis deposition of ZnO thin films on FTO coated substrates from zinc acetate and zinc chloride precursor solution at different growth temperatures, *Journal of Physics and Chemistry of Solids* **72** (2011) 701, https://doi.org/10.1016/j.jpcs.2011.02.017.
18. S. A. Khan, *et al.*, Enhanced photoluminescence performance of MoS2 nanostructures after amalgamation with ZnO NPs, *Optik* **220** (2020) 165201, https://doi.org/10.1016/j.ijleo.2020.165201.
19. W. Yi, *et al.*, Tunable emission in ZnO/Bi2O3 nanocomposites, *Materials Letters* **277** (2020) 128326, https://doi.org/10.1016/j.matlet.2020.128326.
20. D. Bao, H. Gu, and A. Kuang, Sol-gel-derived c-axis oriented ZnO thin films, *Thin solid films* **312** (1998) 37, https://doi.org/10.1016/S0040-6090(97)00302-7.
21. N. S. Kumar, K. V. Bangera, and G. Shivakumar, Effect of annealing on the properties of Bi doped ZnO thin films grown by spray pyrolysis technique, *Superlattices and Microstructures* **75** (2014) 303, https://doi.org/10.1016/j.spmi.2014.07.019.
22. K. Salim, M. N Amroun, and W. Azzaoui, Influence of Doping Concentration on the Properties of Tin Doped Zinc Oxide Thin Films Prepared by Spray Pyrolysis for Photovoltaic Applications, *International Journal of Thin Film Science and Technology* **10** (2021) 9, https://dx.doi.org/10.18576/ijtfst/100309.
23. E. Sarica and V. Bilgin, Structural, optical, electrical and magnetic studies of ultrasonically sprayed ZnO thin films doped with vanadium, *Surface and Coatings Technology* **286** (2016) 1, https://doi.org/10.1016/j.surfcoat.2015.12.008.
24. R. Pandey, *et al.*, Fabrication of aluminium doped zinc oxide (AZO) transparent conductive oxide by ultrasonic spray pyrolysis, *Current Applied Physics* **12** (2012) S56, https://doi.org/10.1016/j.cap.2012.05.027.
25. URL: https://www.bruker.com/products/x-ray-diffraction-and-elementalanalysis/x-raydiffraction/xrd-software/eva.html.
26. P. Shankar, *et al.*, Boron induced c-axis growth and ammonia sensing signatures of spray pyrolysis deposited ZnO thin films-Relation between crystallinity and sensing, *Thin Solid Films* **746** (2022) 139126, https://doi.org/10.1016/j.tsf.2022.139126.
27. H. Cao, *et al.*, Preparation and characterization of Al and Mn doped ZnO (ZnO:(Al, Mn)) transparent conducting oxide films, *Journal of Solid State Chemistry* **177** (2004) 1480, https://doi.org/10.1016/j.jssc.2003.11.030.
28. A. Nakrela, *et al.*, Site location of Al-dopant in ZnO lattice by exploiting the structural and optical characterisation of ZnO: Al thin films, *Results in Physics* **6** (2016) 133, https://doi.org/10.1016/j.rinp.2016.01.010.
29. H. Benzarouk, *et al.*, Effect of the precursor solution on the structural morphological and optical properties of ZnO thin films deposited by Spray Pyrolysis technique for solar cell application, *TC* **2** (2019) 1, https://doi.org/10.1016/j.ceramint.2014.01.048.
30. R. Mimouni, *et al.*, Effect of Mn content on structural, optical, opto-thermal and electrical properties of ZnO: Mn sprayed thin films compounds, *Journal of Alloys and Compounds* **645** (2015) 100, https://doi.org/10.1016/j.jallcom.2015.05.012.
31. A. Badawi, *et al.*, A comparative study of the structural and optical properties of transition metals (M= Fe, Co, Mn, Ni) doped ZnO films deposited by spray-pyrolysis technique for optoelectronic applications, *Optical Materials* **124** (2022) 112055, https://doi.org/10.1016/j.optmat.2022.112055.
32. M. N Amroun, K. Salim, and A. H Kacha, Molarities Effect on Structural Optical and Electrical Properties of Nanostructured Zinc Oxide deposited by Spray Pyrolysis Technique, *International Journal of Thin Film Science and Technology* **10** (2021) 67, https://dx.doi.org/10.18576/ijtfst/100110.
33. N. Chahmat, *et al.*, Structure, microstructure and optical properties of Sn-doped ZnO thin films, *Journal of alloys and compounds* **593** (2014) 148, https://doi.org/10.1016/j.jallcom.2014.01.024.

34. R. Miloua, *et al.*, Determination of layer thickness and optical constants of thin films by using a modified pattern search method, *Optics letter*s **37** (2012) 449, https://doi.org/10.1364/OL.37.000449.

35. M. Miki-Yoshida, *et al.*, Influence of Al, In, Cu, Fe and Sn dopants on the response of thin film ZnO gas sensor to ethanol vapour, *Thin Solid Films* **373** (2000) 137, https://doi.org/10.1016/S0040-6090(00)01120-2.

36. A. Babar, *et al.*, Gallium doping in transparent conductive ZnO thin films prepared by chemical spray pyrolysis, *Journal of Physics D: Applied Physics* **41** (2008) 135404, https://doi.org/10.1088/0022-3727/41/13/135404.